RSC Advances

RSC Advances RSCPublishing

PAPER

Surface-enhanced Raman Scattering (SERS) Chips Made by Metal Nanoparticles Doped Polymer Fibers

Cite this: DOI: 10.1039/x0xx00000x

Wenran Gao, Gang Chen, Weiqing Xu, Chenggong Yang, Shuping Xu*

Received 00th January 2012,
Accepted 00th January 2012

DOI: 10.1039/x0xx00000x

www.rsc.org/

We employed the electrospinning method to prepare metal nanoparticles (NPs) doped polymer nanofiber mats, which can be easily cut into a proper size and fixed on slides or microfluid channels to work for surface-enhanced Raman scattering (SERS) measurements. Metal NPs embedded in the composite nanofibers maintained their intrinsic shape and monodispersity, as well as enhancement ability. In addition, they can be re-suspended into aqueous solution to recover a colloidal solution with persistent SERS activity. The SERS chips made by the metal NPs doped polymer nanofiber mats displayed high detection sensitivity and reproducibility. The microfluid chips decorated by several metal NPs doped polymer nanofiber mats possess multi-SPR properties and can be widely optional for different analytes. These composite polymer mats facilitate storage and transportation, which also possess possible practicality as antibacterial filter and paint for medical purposes.

1. Introduction

Metal colloidal nanoparticles (NPs) gain great interests due to their abundant applications in the fields of biochemical sensing,[1–3] optoelectronic devices,[4] photocatalysis[5] and surface-enhanced spectroscopy,[6–8] thermal medication[9,10] etc. These applications are all based on the surface plasmon resonance (SPR) properties of metal colloidal NPs, which can enlarge the effective scattering cross section over their geometric shapes, causing the enhanced efficiencies of light harvesting and radiation. The SPR effect behaves most obviously in terms of surface-enhanced Raman scattering (SERS), answering for million-fold enhancement to Raman signal. Of course, SERS measurements strongly and strictly depend on the SPR properties of metal NPs, requiring the exact matching of SPR band and excitation wavelength.

Besides spherical metal particles, many anisotropic metal NPs have been introduced to act as SERS substrates due to their rich SPR characteristics, such as gold nanorods,[11] silver nanoprisms,[12] silver nanocubes[13] and etc. Meanwhile, a variety of techniques strived for the controllable adjustment of SPR properties of anisotropic metal NPs in a wide (or proper) spectral range, for example, changing respect ratio (gold rods) by different reaction conditions,[14] shape transformation by adding etching reagents,[15,16] dominating by wavelength self-limiting effect in laser–induced growth[17] and so on. To widen the applicability and stability of metal colloidal NPs as SERS substrates, these particles have been combined with solid-supported slides[18–21] or bulky substances (e.g. vials,[20] capillaries,[20] optical fibers,[22] porous anodic alumina,[23] and etc[24-26]) to achieve highly stable and active SERS chips. These SERS chips have distinct advantages of easy carry and storage. Strategies for building SERS chips by metal colloidal NPs are various. The assembly methods based on supramolecular interaction or covalent bond are usually adopted, which require the surface modification of metal NPs or chip substrates by silicone agents[18] or polyelectrolyte.[19] Owing to different surface functional groups of various colloidal NPs, finding a universal combination strategy is still a challenge.

Electrospinning technique can satisfy the strict requirement of universality. It can obtain composite fibrous mats in high efficiency and make metal NPs combination feasible. In this study, electrospinning technique has been employed to prepare metal NPs doped polymer nanofiber mats. Further, these composite polymer mats were cut into a proper size and fixed on a slide or a microfluid chip to fabricate multi-SPR functionalized chips. These metal NPs doped polymer nanofibers are responsible for SERS enhancement. When measuring SERS on the multi-SPR functionalized chips, laser wavelength is optional to match the resonance of metal NPs, ensuring the highest SERS.

2. Experimental Section

2.1 Materials

Silver nitrate ($AgNO_3$, 99.8%) and chloroauric acid ($HAuCl_4 \cdot 4H_2O$, Au content >47.8%) were purchased from Shanghai Reagent No.1 Plant. $NaBH_4$ (96%) and polyvinyl pyrrolidone (PVP) (Mw=30000) were obtained from Sinopharm Chemical Reagent Co., Ltd. Trisodium citrate (99.0%) and 4-mercaptobenzoic acid (4-MBA) were supplied by the Beijing Chemical Reagent Plant. Polyvinyl alcohol (PVA, Mw=130000), 4-mercaptopyridine (4-MPY), Atto 610-biotin and hexadecyltrimethylammonium bromide (CTAB) were purchased from Sigma-Aldrich. Rhodamine 6G (R6G) was obtained from Exciton Chemical Co. Inc. Teflon tape was purchased from Tianjin Tiansu Science &Technology Group Co., Ltd. PMMA mass was obtained from Foshan City Shunde Jundao Optical Sheet Manufacturing Co., Ltd.

2.2 Preparation of Metal NPs Doped Polymer Fibers

Firstly, to obtain metal NPs doped polymer fibers with multiple SPR bands, we prepared several kinds of metal NPs, involving Au/Ag NPs with different shape and size. Colloidal Au nanospheres with different size were synthesized by the method of Frens.[27] The size of Au particles was controlled by the amount of trisodium citrate. Au nanorods were prepared by the seed-mediated growth method.[14] Silver nanospheres were prepared by the Lee method.[28] These metal NPs were concentrated to 120 times by centrifuge before further use while PVP was added as a stabilizer (0.1 g of PVP for 100 mL of metal colloid).

Secondly, metal NPs doped polymer fibers were prepared by electrospun. Electrospinning solutions containing 0.8 mL of concentrated metal NPs and 0.08 g of PVA were prepared with stirring and heating (70 ℃) by a magnetic stirring heater. In a typical electrospinning process, the electrospinning solution was kept in a plastic syringe (capacity of 1.0 mL) with a metal needle. The applied voltage was 15 kV. A distance of 15 cm was set between the tip of the metal needle and the collector of the aluminum foil. The flow rate for the electrospinning solution was 0.2 mL/h. The metal NPs doped polymer fiber mats were obtained after 4hrs of electrospinning.

2.3 Fabrication of SERS Chips by Using Metal NPs Doped Polymer Fibers.

Two types of SERS chips were fabricated specially for testing analytes in organic solvents (SERS chip Ⅰ) and in water (SERS chip Ⅱ), respectively. SERS chips Ⅰ were constructed by the metal NPs doped polymer fiber mats (cut into 3 mm×3 mm). To test the analytes in organic solvents, the metal NPs doped polymer fiber mats were immersed in sample solutions for the desired time (several hours) and then dried at room temperature before Raman measurements. SERS chip Ⅱ is made by laying a piece of metal NPs doped polymer mat (3 mm × 3 mm) on a hydrophobic membrane (Teflon tape) decorated glass slide. To detect SERS signal by SERS chip Ⅱ, 15 μL of sample aqueous solution was dripped on it and then dried.

In addition, several metal NPs doped polymer fiber mats were cut into narrow belts to decorate the microfluidic channels to fabricate the microfluidic SERS chip with multi-SPR function. Microfluidic channels were engraved by an engraving machine on a PMMA mass.

2.4 characterizations

Ultraviolet–visible (UV–vis) absorption spectra of metal colloidal solutions were measured by a Shimadzu UV-3100 and an Ocean Optics USB2000 spectrophotometers. Field-emission scanning electron microscope (SEM, HITACHI SU8000) and Transmission electron microscope (TEM, JEOL JEM-2100F) were employed to investigate the morphologies of metal NPs doped polymer fibers. A confocal Raman system (LabRAM ARAMIS, Horiba Jobin-Yvon) with a ~0.7 μm spatial resolution, and a 5 mW, 633 nm HeNe laser as excitation sources, was used for the collection of Raman spectra. The detection of Raman signal was carried out with a Synapse Thermoelectric cooled charge-coupled device (CCD) camera (Horiba Jobin-Yvon). Raman scattering light was collected with a 50 × microscope objective lens (0.50 NA, LMPLFLN, Olympus, Japan) that was also used for focusing the excitation laser light. The laser beam focusing on the tissue formed a spot with the diameter of 1.5 μm. The strong Rayleigh-scattered lights were then blocked by a 4-notch filter (HORIBA JOBIN YVON, EDISON, NJ, USA). Extended scan spectra with a spectral range of 300-1800 cm^{-1} were acquired using an integration time of 10 s and 2 accumulations. The wavenumber calibration was set by reference to the 520.7 cm^{-1} vibrational band of a silicon wafer.

To compare the SERS signals obtained under different excitation wavelengths, a portable BWTEK Raman spectrometer with 532 nm excitation wavelength was used. The integration time was 10 s. The laser power reaching the samples was 1.32 mW. The scan range was of 300−1800 cm^{-1}. Three different points from each sample were chosen, and the data were the average values of three times.

3. Results and Discussion.

3.1 Characterizations of Metal NPs Doped Polymer Fibers.

Five types of metal NPs were employed to fabricate the metal NPs doped polymer composite fibers. Three of them are Au spheres with different sizes (13, 16, and 40 nm) and the other two are Ag NPs and Au nanorods. Panel (1) of Figure 1 shows the TEM images of the prepared colloidal metal NPs. It can be observed that metal NPs were mostly uniform in sizes and shapes except Ag NPs. When metal NPs were combined with PVA fibers by electrospinning, they needed to be concentrated to about 125 times even above to ensure their density in polymer fibers high enough for SERS enhancment requirement. However, too higher metal NP density will cause the aggregation of metal NPs and also affect the mechanics of PVA fibers, causing the failure of electrospinning. Panel 2 of Figure 1 displays the TEM images of metal NPs doped PVA

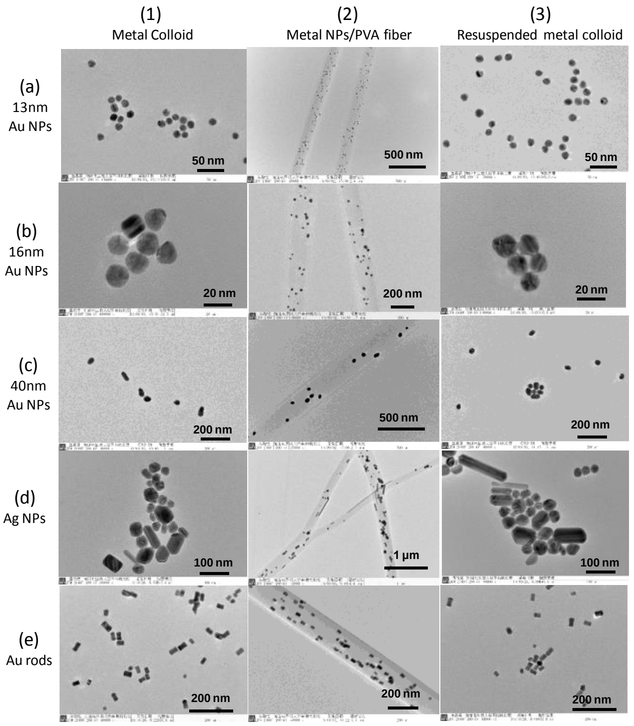

Figure 1. TEM images of five kinds of the prepared metal NP colloids (left panel), the metal NPs doped PVA nanofibers obtained by electrospinning (middle panel) and the metal NPs obtained by resuspending metal NPs/PVA nanofibers in water (right panel).

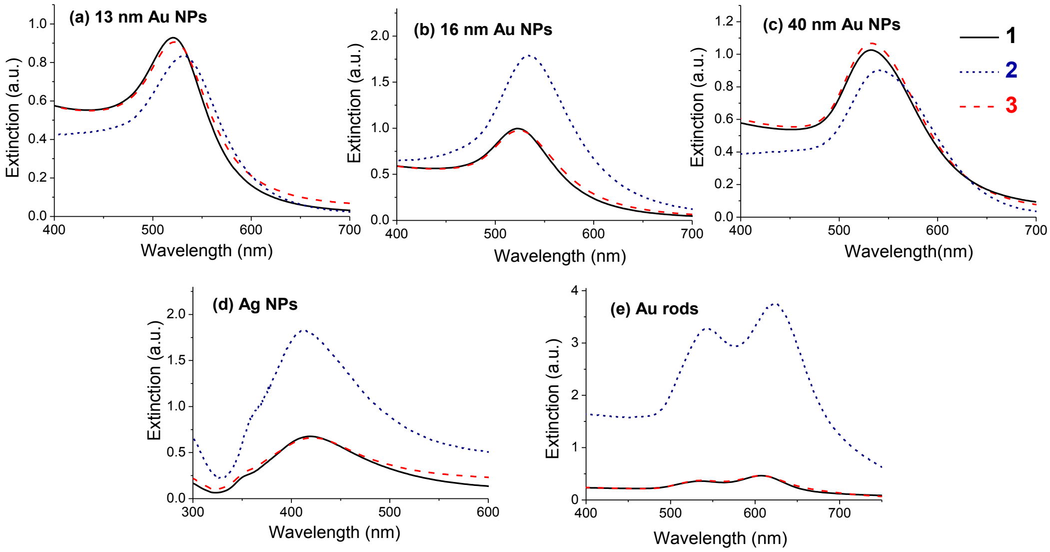

Figure 2. Extinction spectra of the prepared metal NP colloids (1; solid line), metal NPs doped PVA nanofibers (2; short dash line) and the metal NPs obtained by resuspending metal NPs doped PVA nanofibers in water (3; dash line).

Table 1. A summary of the sizes, shapes and extinction band positions of metal NPs at different forms.

Metal NPs	Shape	Size/nm	Band position/nm 1 Metal colloid	 2 Metal NPs/PVA fiber	 3 Resuspended metal colloid in water
Au NPs	Sphere	13	521	532	522
Au NPs	Sphere	16	523	534	524
Au NPs	Sphere	40	533	541	533
Ag NPs	Irregular shape	~43	418	412	418
Au rods	Rod	31 in width, 20 in length	535, 607	542, 622	535, 607

fibers. It can be observed that most of metal NPs were well dispersed and doped in PVA fibers and some of them were semi-embedded in the PVA fibers. Interestingly, owing to the high inducing voltage applied on these electrospinning solutions, rod or stick typed metal NPs were aligned with the polymer fibers (Images d-2 and e-2). Figure 2 shows the extinction spectra of these metal colloids (solid lines) and their corresponding composite polymer nanofibers (short dash lines). Table 1 summarizes the details of metal NPs' morphologies and their extinction band positions as observed in Figure 1 and 2. By comparison, it is found that the extinction band positions of the metal NPs doped polymer fiber mats have red-shifts toward their colloid systems, except that Ag NPs doped polymer fiber mat has a tiny blue-shift. These shifts are mainly because the surrounding mediums around metal NPs varied when they were combined with PVA.

Figure 3 shows the SEM images of metal NPs doped polymer fibers. We can see that the average diameters of metal NPs doped polymer fibers are 260~300 nm and the lengths extend to several millimetres or more. The metal NPs doped polymer fibers interlaced and show a 3-dimensational network. The insets are the pictures of metal NPs doped polymer fibers and metal NP solutions. It is observed that metal NPs doped polymer fiber mats exhibit the same colours as their metal NPs solutions, which has been proved by their extinction spectra (Figure 2).

The polymer we used to electrospin is PVA and it is a water-soluble polymer. We resuspended the metal NPs doped polymer fibers into water, achieving the metal colloids again. The TEM images (Panel 3 of Figure 1) of the resuspended metal colloids prove that these metal NPs can be well re-dispersed in water. The extinction spectra of the resuspended metal colloids were also provided (dash lines in Figure 2). Compared with the fresh prepared metal colloids (solid lines), their plasmonic bands have no difference. It means no metal aggregates are found during the electrospinning process and their SERS activity still remains (see ESI). These results indicate the electrospinning process has no harm to the stability of colloidal metal NPs. This is especially important for SERS measurements because the uncontrollable aggregation of colloidal metal NPs will lead to the poor reproducibility in SERS detections and this method avoids this.

Metal NPs combined with bulky materials show long-term stability. There are almost no changes after stored for 6 months (see ESI). The long-term stability ensures that these metal NPs doped polymer fiber mats are promising for the commercial use.

3.2 Fabrication of SERS chips and their SERS applications.

3.2.1 SERS CHIP Ⅰ FOR PROBING ANALYTES IN ORGANIC SOLUTIONS.

PVA is resistant to organic solvents and easy to dissolve in water. Thus, we first designed SERS chip Ⅰ for measuring

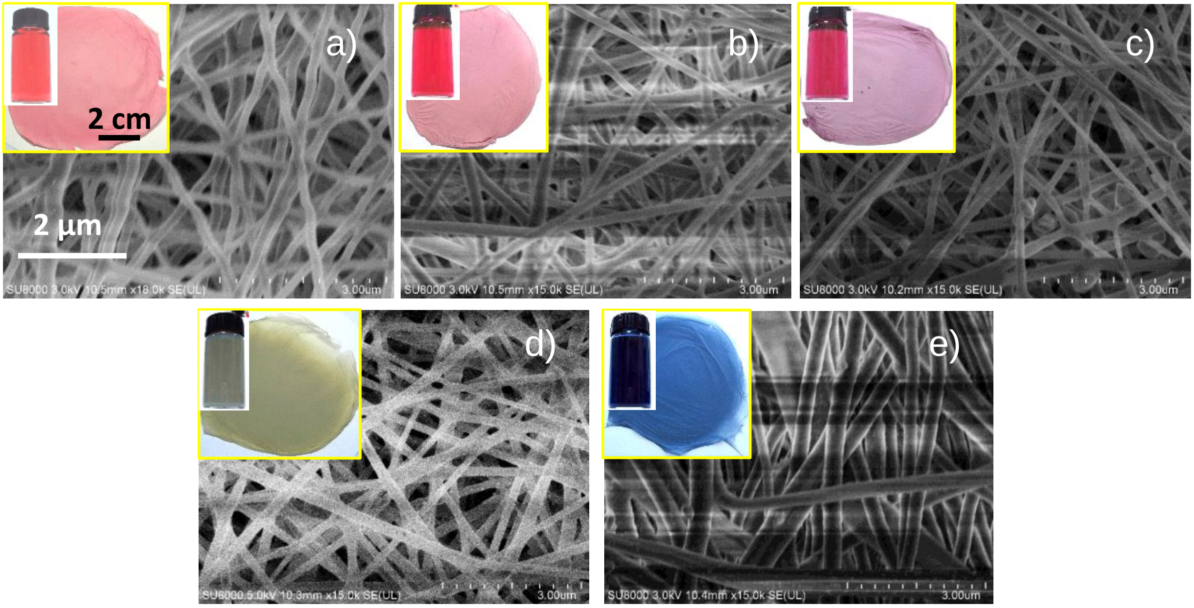

Figure 3. SEM images of five kinds of metal NPs doped polymer fibers. a-e correspond to 13, 16 and 40 nm Au NPs, Ag NPs and Au nanorods, respectively. Insets show the photos of metal colloids and metal NPs doped polymer fiber mats.

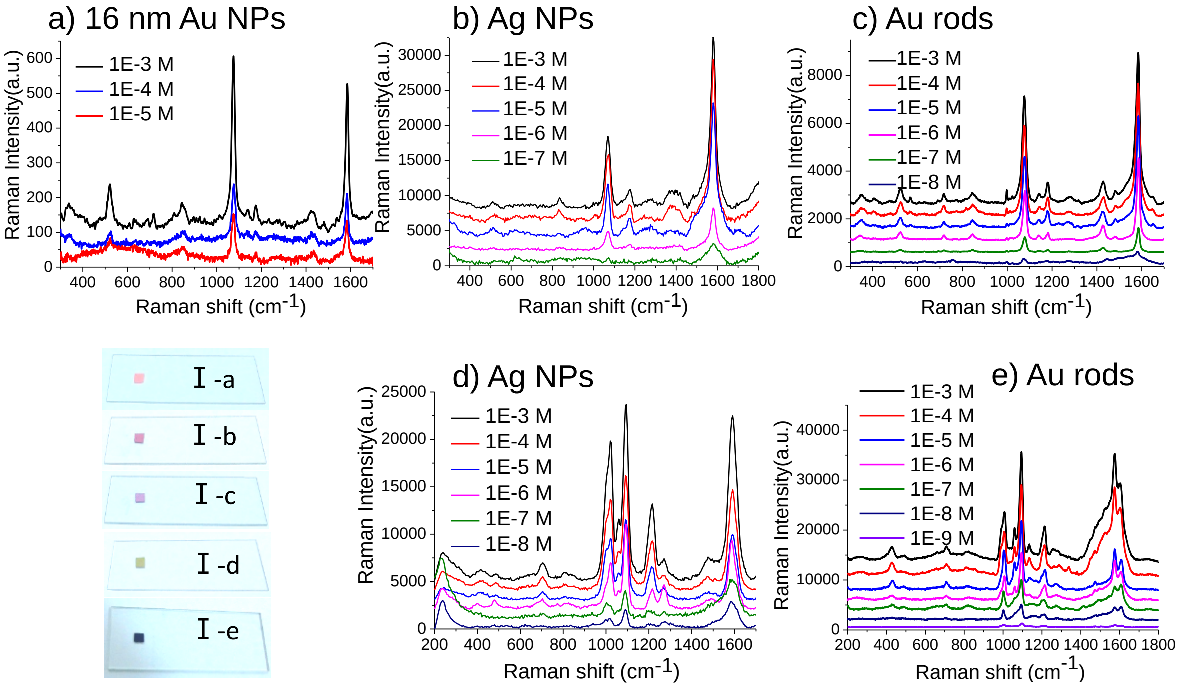

Figure 4.Concentration-dependant SERS detections of 4-MBA (a, b and c) and 4-MPY (d and e) by using the SERS chip Ⅰ under the excitation wavelengths of 633 (a, c and e) and 532 nm (b and d). The photos of five SERS chips Ⅰ are provided, corresponding to 13, 16 and 40 nm Au NPs, Ag NPs and Au nanorods, respectively.

analytes in organic solutions. Figure 5 displays the photos of SERS chip Ⅰ, which are made by five pieces of 3 mm×3 mm metal NPs doped PVA fiber mats on glass slides. 4-MBA and 4-MPY were used as probed molecules to evaluate the SERS enhancement effect of these SERS chips. They were dissolved in ethanol solutions to desired concentrations. When the SERS chip Ⅰ was immersed in the ethanol solution, probed molecules can permeate into the polymer fibers and access to the metal NPs. Finally, probing molecules will adsorb onto the surface of metal NPs. It should be noted that the integrality of SERS chip Ⅰ is retained during SERS measurements in this case.

Figures 4 a-c show SERS detections of 4-MBA using different SERS chips Ⅰ constructed by Au NPs (16 nm), Ag NPs and Au rods, with the trace levels of 1.0×10^{-5}, 1.0×10^{-7} and 1.0×10^{-8} M, respectively. To determine 4-MPY, the trace levels of 4-MPY using Ag NPs and Au nanorods doped polymer fibers are 1.0×10^{-8} and 1.0×10^{-9} M (Figures 4 d and

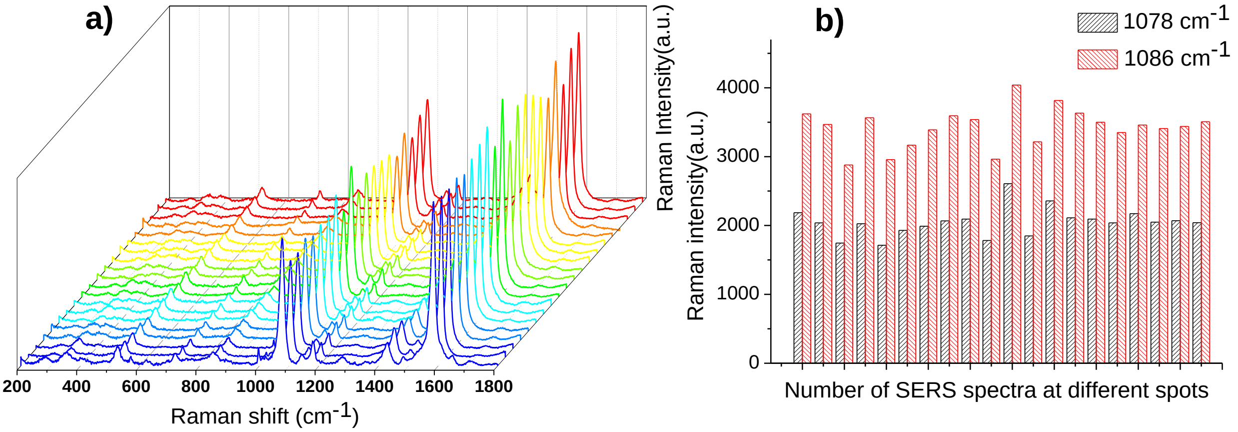

Figure 5. a) SERS spectra of 4-MBA (1.0×10^{-5} M) adsorbed on the Au nanorods/PVA nanofibers under 633 nm excitation from randomly selected 20 spots. b) The intensities of two different peaks at 20 spots on the same substrate.

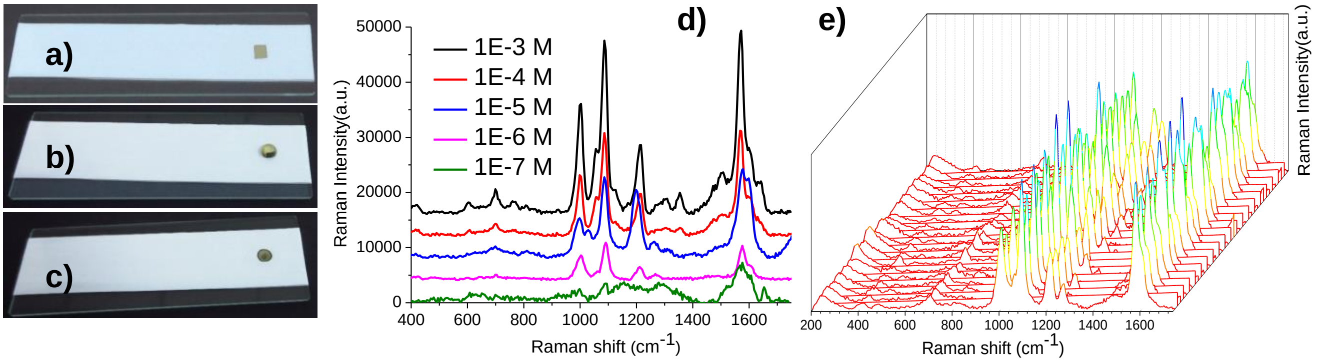

Figure 6. The pictures of SERS chips Ⅱ and their SERS detections. a) A Ag NPs/PVA fiber mat on a hydrophobic surface. b) A 15 μL of sample aqueous solution was dropped on the Ag NPs/PVA fiber mat. c) Sample solution was dried and a circle of stain containing Ag NPs, PVA and analytes was left on the hydrophobic surface. d) SERS determination of 4-MPY aqueous solutions at different concentrations (1.0×10^{-3} to 1.0×10^{-7} M) by SERS chips Ⅱ. e) SERS spectra of 4-MPY aqueous solution (1.0×10^{-5} M) tested by SERS chip Ⅱ from randomly selected 20 points. The excitation laser was 532 nm.

e). These results show that SERS chips Ⅰ provide acceptable SERS enhancement activity.

In addition, we investigated the reproducibility of the SERS chip Ⅰ by comparing SERS signals from 20 different spots on the same SERS chip (Figure 5a). Two peaks at 1078 cm^{-1} and 1086 cm^{-1} are chosen to evaluate the reproducibility of this SERS chip (Figure 5b). The relative standard deviations of spot to spot of Raman intensities are 10% and 8.3% in Figure 5b, which prove SERS chip Ⅰ exhibits preferable reproducibility to the scientific standard of SERS substrates in which less than 20% spot-to-spot variation over 10 mm2 is required.[29]

3.2.2 SERS CHIP Ⅱ FOR PROBING ANALYTES IN AQUEOUS SOLUTIONS.

SERS chip Ⅰ can only test organic solution samples and cannot work for water solutions because PVA is water soluble. To solve this problem, we modified the glass slide with a hydrophobic surface to support the metal NPs doped PVA fiber mats, which is named as SERS chip Ⅱ (Figure 6a). Thus, when dripping a drop of water sample (15 μL) on the SERS chip Ⅱ, the water drop can be hold in a very restricted region (Figure 6b). At the same time, the analytes can easily access to metal NPs during the dissolving process of PVA fibers. Figure S3 in ESI display a SEM image of the surface after a 4-MPY aqueous solution was dripped on SERS chip II and dried. The PVA fibers were totally destroyed and they formed a flat film with metal NPs and 4-MPY doped inside. We measured SERS signal of analytes when the water drop was dry (Figure 6c). Figure 7d shows that the trace level of 4-MPY on SERS chip Ⅱ is 1.0×10^{-7} M. Comparing the trace level, SERS chip Ⅰ is better than SERS chip Ⅱ. The relative standard deviation of spot to spot of Raman intensity is 16.9% (data from Figure 6e), which is also a little higher than SERS chip Ⅰ. The relatively lower enhancement activity and reproducibility might be caused by the uneven surface (or metal NP density) forming when the droplet drying.

3.2.3 DECORATION OF MICROFLUIDIC CHANNELS WITH MULTI-SPR PROPERTY.

The choice of excitation wavelength is very important for SERS measurements because it not only affects the coupling efficiency of the plasmonic bands of metal NPs, but also decides the resonance effect of probed molecules. Here, we chose two kinds of analytes, R6G and Atto 610-biotin. Their absorption bands locate at 523 and 615 nm (dash lines in Figures 7a and 7c), which are close to the laser excitation

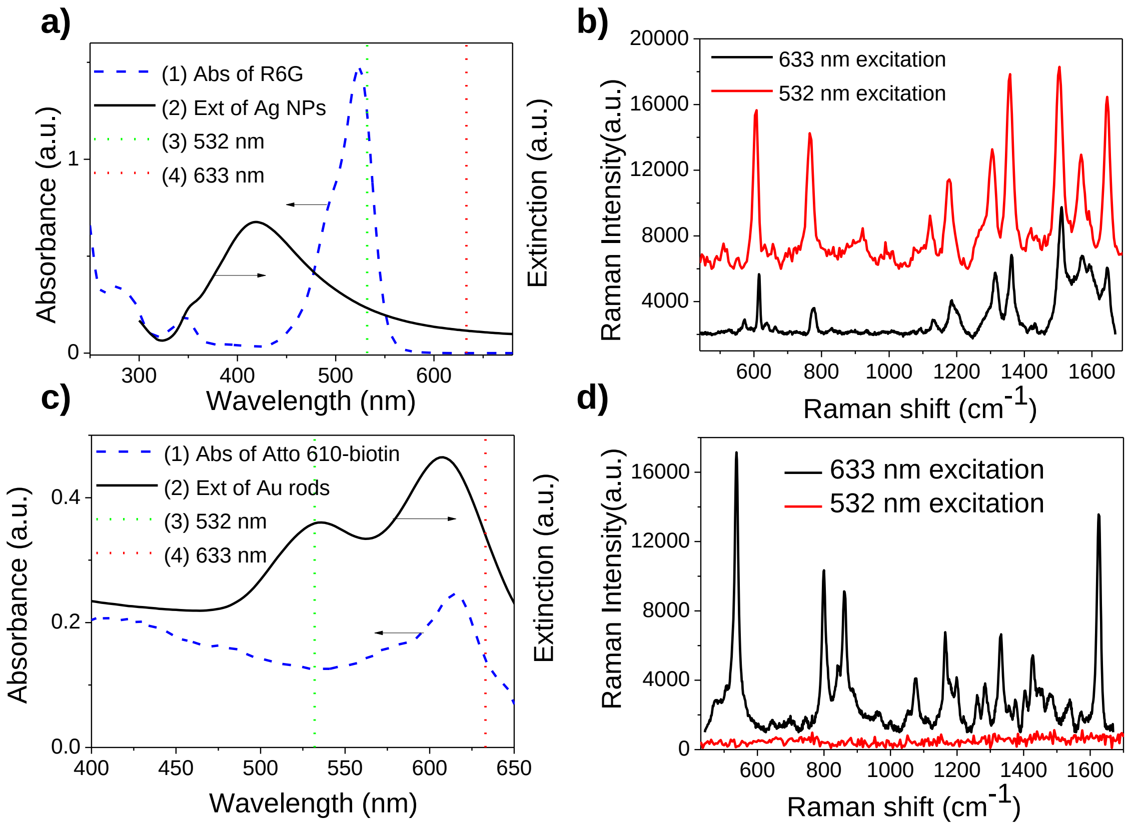

Figure 7. a) The UV-Vis absorption spectrum of a R6G ethanol solution (1×10^{-7} M) and the extinction spectrum of colloidal Ag NPs. b) SERS spectra of R6G (1×10^{-6} M, ethanol solution) obtained on the Ag NPs/PVA nanofibers under different excitation wavelengths. c) The UV-Vis absorption spectrum of an Atto 610-biotin ethanol solution (1×10^{-4}mg/mL) and the extinction spectrum of colloidal Au nanorods. b) SERS spectra of Atto 610-biotin (1×10^{-4} mg/mL, ethanol solution) obtained on the Au nanorods/ PVA nanofibers under different excitation wavelengths.

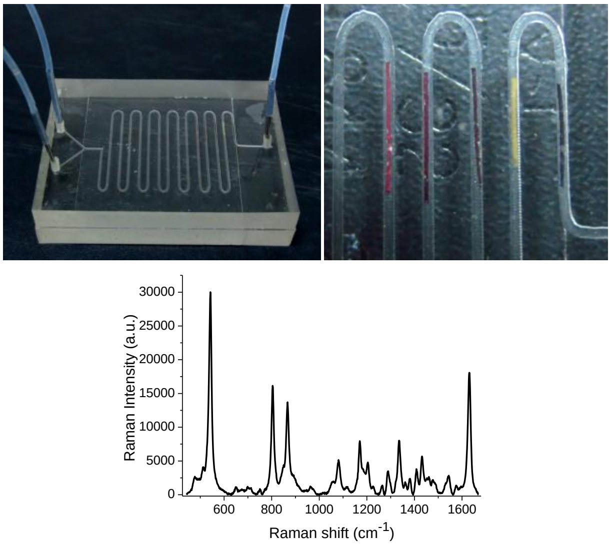

Figure 8. The pictures of a SERS microfluid chip decorated with several kinds of metal NPs doped polymer fibers (top) and the SERS detection of Atto 610-biotin (1×10^{-4} mg/mL, ethanol solution) in the SERS microfluid chip (bottom). For comparison, a Raman spectrum of the microfluid (PMMA) is provided in ESI.

wavelengths of 532 and 633 nm (dot lines), respectively. When we chose suitable wavelengths to excite these probed molecules, the resonance effect of dye molecules will be involved. Figure 8b displays the SERS and surface-enhanced resonance Raman spectrum (SERRS) of R6G on the Ag NPs/PVA nanofibers, corresponding to the excitation wavelengths of 633 and 532 nm. The reason why we adopted the Ag NPs/PVA fibers for R6G measurement is based on their predominant SERS enhancement ability under green laser due to the presence of plasmonic coupling (solid line in Figure 7a). As we expected, SERRS signal under 532 nm excitation is higher than SERS signal under 633 nm excitation, which proves that the resonance effect of dyes and the plasmonic coupling of Ag NPs support higher signal. Owing to the same reasons, the detection of Atto 610-biotin (Figure 7d) shows that SERRS signal under 633 nm excitation is much higher. In latter case, the Au nanorods/PVA fibers were used, which supported the plasmonic resonance with 633 nm laser (solid line in Figure 7c). These two trials illuminate that when we pursue highest signal in SERS detections, we need to consider about many factors including excitation wavelength and electron energy bands of probed molecules and how to maximize the effects of these factors. This requires a programming SERS substrate with designed plasmonic property. For the sake of a wide choice, a multi-SPR functionalized chip is needed.

To achieve this, the metal NPs doped polymer fiber mats by electrospun method can satisfy above requirement and have the advantages of high efficiency and broad applicability for the combination of metal NPs. These composite polymer mats were cut into a proper size and fixed on a PMMA microfluid chip to fabricate multi-SPR functionalized SERS chips. Figure 8 is the photo picture of the SERS microfluid chip made by metal NPs doped polymer fibers. We decorated the microfluid channels with different metal NPs doped polymer fibers. An example of SERS detection of Atto 610-biotin under 633 nm excitation using this SERS microfluid chip made by Au nanorods doped polymer fibers is provided. It is noted that ethanol solvent and the chip material PMMA both exhibit relatively weak spectral signals comparing to the signal of Atto-610 (see Figure S4 and S5 in ESI) and show little spectral interference. This multi-SPR functionalized SERS microfluid chip owns great merits in the SERS determinations of complicated and multicomponent systems.

4. Conclusions

In summary, we successfully prepared metal NPs doped polymer fibers by electrospun method. Electrospinning technique is a universal and flexible approach to combine metal NPs with bulky materials in high efficiency. Metal NPs were well dispersed in the polymer fibers and displayed persistent SERS activity. The metal NPs doped polymer fibers are free-standing, flexible, and extraordinarily stable. Furthermore, two types of SERS chips made by metal NPs doped polymer fiber mats (SERS chip Ⅰ and SERS chip Ⅱ) were fabricated for probing analytes in organic and aqueous solutions. SERS detection results show that both types of SERS chips have good SERS enhancement activity and acceptable reproducibility. In addition, these composite polymer mats were fixed in a microfluid chip to fabricate multi-SPR functionalized chips, which are applicable for the SERS determinations of complicated and multicomponent systems. These composite polymer mats facilitate storage and transportation. They can also be applied in medical fields, e.g. as a colourful antibacterial filter and paint. Relative study is underway.

5. Acknowledgements

This work was supported by the National Natural Science Foundation of China (No. 21373096, 21073073 and 91027010), the Ministry of Education of returned overseas students to start research and fund projects and the National Instrumentation Program (NIP) of the Ministry of Science and Technology of China no. 2011YQ03012408. We thank Prof. Kun Liu, Jilin University for the sample supply of Au nanorods and Prof. Ce Wang, Jilin University for teaching us electrospinning technique.

6. Notes and references

State Key Laboratory of Supramolecular Structure and Materials, Jilin University, Changchun130012, P. R. China. Email:xusp@jlu.edu.cn

† Electronic Supplementary Information (ESI) available: (1) SERS spectra obtained from Au NP colloids or the dissolved Au NPs/PVA fibers on glass substrates under 633 nm excitation. (2) Extinction spectra of five kinds of metal NPs doped polymer fibers before and after 6 months storage. (3) SEM image of SERS chip (II) after a 4-MPY aqueous solution was dripped on and dried. (4) SERS spectrum of PMMA under 633 nm excitation. (5) SERS spectrum of ethanol under 633 nm excitation. See DOI: 10.1039/b000000x/

1. K. A. Willets and R. P. Van Duyne, Annu. Rev. Phys. Chem., 2007, 58, 267–297.
2. C. A. Mirkin, R. L. Letsinger. R. C. Mucic and J. J. Storhoff, Nature, 1996, 382, 607-609.
3. M. Lismont and L. Dreesen, Mater. Sci. Eng. C, 2012, 32, 1437–1442.
4. J.-L. Wu, F.-C. Chen, Y.-S. Hsiao, F.-C. Chien, P. Chen, C.-H. Kuo, M. H. Huang, and C.-S. Hsu, ACS Nano, 2011, 5, 959–967.
5. P. V. Kamat, J. Phys. Chem. B, 2002, 106, 7729–7744.
6. J. A. Creighton, C. G. Blatchford, and M. G. Albrecht, J Chem Soc Faraday Trans 2, 1979, 75, 790–798.
7. Y. C. Cao, R. C. Jin and C. A. Mirkin, Science, 2002, 297, 1536–1540.
8. M. Moskovits, Rev. Mod. Phys., 1985, 57, 783.
9. D. P. O'Neal, L. R. Hirsch, N. J. Halas, J. D. Payne, and J. L. West, Cancer Lett., 2004, 209, 171–176.
10. X. Huang, I. H. El-Sayed, W. Qian, and M. A. El-Sayed, J. Am. Chem. Soc., 2006, 128, 2115–2120.
11. C.-L. Zhang, K.-P. Lv, H.-P. Cong, and S.-H. Yu, Small, 2012, 8, 648–653.
12. M. Liu, Z. Wang, S. Zong, R. Zhang, D. Zhu, S. Xu, C. Wang, and Y. Cui, Anal. Bioanal. Chem., 2013, 405, 6131–6136.
13. H. K. Lee, Y. H. Lee, Q. Zhang, I. Y. Phang, J. M. R. Tan, Y. Cui, and X. Y. Ling, ACS Appl. Mater. Interfaces, 2013, 5, 11409–11418.
14. B. Nikoobakht and M. A. El-Sayed, Chem. Mater., 2003, 15, 1957–1962.
15. J. An, B. Tang, X. L. Zheng, J. Zhou, F. X. Dong, S. P. Xu, Y. Wang, B. Zhao, and W. Q. Xu, J. Phys. Chem. C, 2008, 112, 15176–15182.
16. S. P. Xu, B. Tang, X. L. Zheng, J. Zhou, J. An, X. H. Ning, and W. Q. Xu, Nanotechnology, 2009, 20, 415601.
17. X. L. Zheng, W. Q. Xu, C. Corredor, S. P. Xu, J. An, B. Zhao, and J. R. Lombardi, J. Phys. Chem. C, 2007, 111, 14962–14967.
18. R. G. Freeman, K. C. Grabar, K. J. Allison, R. M. Bright, J. A. Davis, A. P. Guthrie, M. B. Hommer, M. A. Jackson, P. C. Smith, D. G. Water and M. J. Natan, Science, 1995, 267, 1629-1630.
19. X. L. Li, W. Q. Xu, J. H. Zhang, H. Y. Jia, B. Yang, B. Zhao, B. F. Li, and Y. Ozaki, Langmuir, 2004, 20, 1298–1304.
20. http://www.rta.biz
21 http://www.pers-spec.org
22 W. Q. Xu, S. P. Xu, B. Hu, K. X. Wang, B. Zhao, Y. T. Xie, and Y. G. Fan, Chemical Journal of Chinese Universities, 2004, 25, 144–147.
23 X. N. Wang, S. P. Xu, H. B. Li, J. L. Tao, and W. Q. Xu , J. Raman Spectrosc., 2012, 43, 459–463.
24 L. Zhang, X. Gong, Y. Bao, Y. Zhao, M. Xi, C. Jiang, and H. Fong, Langmuir, 2012, 28, 14433-14440.
25 M. Cao, S. Cheng, X. Zhou, Z. Tao, J. Yao, and L.-J. Fan, Journal of Polymer Research, 2011, 19.
26 X. Li, M. Cao, H. Zhang, L. Zhou, S. Cheng, J.-L. Yao, and L.-J. Fan, Journal of Colloid and Interface Science, 2012, 382, 28–35.
27 J. Frens, Nature physical science, 1973, 241, 20-22.
28. P. C. Lee and D. Meisel, J. Phys. Chem., 1982, 86, 3391–3395.
29. M. J. Natan, Faraday Discuss., 2006, 132, 321–328.

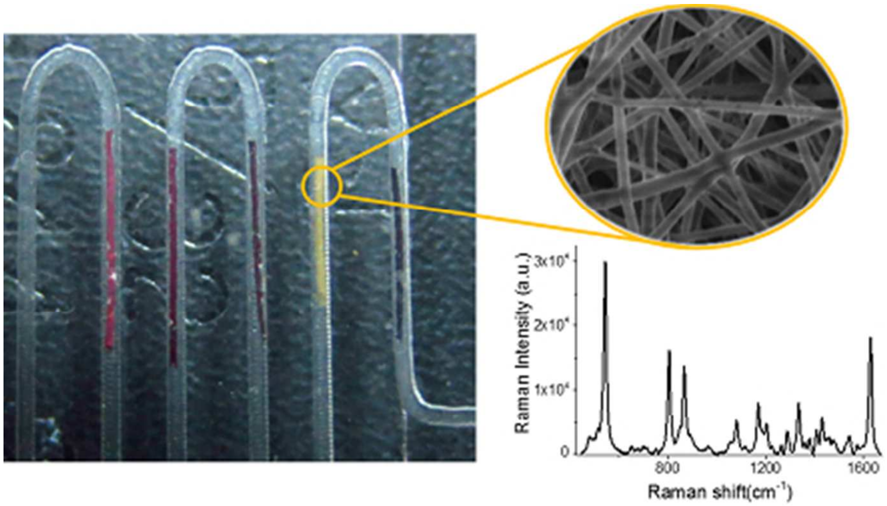
Raman Intensity (a.u.)
3x10⁴
2x10⁴
1x10⁴
0
800
1200
1600
Raman shift(cm⁻¹)